

# Sub-micron dispersed-phase particle size in polymer blends: overcoming the Taylor limit via solid-state shear pulverization

Andrew H. Lebovitz<sup>a</sup>, Klementina Khait<sup>a</sup>, John M. Torkelson<sup>a,b,\*</sup>

<sup>a</sup>*Department of Chemical Engineering, Northwestern University, Evanston, IL 60208-3120, USA*

<sup>b</sup>*Department of Materials Science and Engineering, Northwestern University, Evanston, IL 60208-3120, USA*

Received 8 August 2002; received in revised form 17 September 2002; accepted 19 September 2002

---

## Abstract

A comparison was made of the fineness of dispersion in immiscible polymer blends achieved by a continuous mechanical alloying technique, solid-state shear pulverization, relative to that achieved by melt mixing. Two polymer blend systems were investigated. A polystyrene (PS)/polyethylene (PE) wax blend was studied because, based on a classic analysis by G.I. Taylor, melt mixing was expected to yield a number-average dispersed-phase domain size,  $D_n$ , well above 1  $\mu\text{m}$ . A PS/high density polyethylene (HDPE) blend was also studied because it was known to produce a sub-micron number-average dispersed-phase particle size when mixed by twin-screw extrusion. In the case of the PS/PE wax blend at compositions ranging from 1 to 15 wt% polyethylene wax, pulverization resulted in nearly identical  $D_n$  values (typical value of 0.7  $\mu\text{m}$ ) independent of minor-phase content; these  $D_n$  values were an order of magnitude smaller than the anticipated Taylor limit for melt-mixed blends. In contrast, PS/PE wax blends made by batch, intensive melt mixing yielded  $D_n$  values between  $\sim 3 \mu\text{m}$  at both 1 and 5 wt% minor-phase content and 17.5  $\mu\text{m}$  at 15 wt% minor-phase content. The increase in  $D_n$  with increasing dispersed-phase content in the melt-mixed blend is a consequence of coalescence present during melt processing; such effects are disallowed in the pulverization process occurring in the solid state. Scanning electron microscopy of a 95/5 wt% PS/HDPE blend provided  $D_n$  values of 500 and 270 nm in the twin-screw extruded and pulverized samples, respectively. Fractionated crystallization studies further corroborated the ability of pulverization to result in a finer, nanoscopic dispersion of the minor phase as compared to extrusion.

© 2002 Elsevier Science Ltd. All rights reserved.

**Keywords:** Pulverization; Mechanical alloying; Polymer blends

---

## 1. Introduction

Melt processing of immiscible polymer blends presents many challenges [1–19]. In the typical case, a morphology of droplets of the minority phase in a matrix of the majority phase is desired. In order to achieve the greatest synergy in blend properties, the dispersed-phase domain size often must be maintained at or below a critical size [4]. However, the size of the dispersed-phase domains obtained via conventional melt mixing is strongly influenced not only by blend thermodynamics, such as interfacial tension between blend components [5], but also by the mixing methodology and the viscosity ratio of the blend components [3,6–8], limiting the choice of polymers to be used in producing viable blends. Additionally, there is the

challenge of polymer blend compatibilization [9–14,18,19], related to stabilizing the desired dispersed-phase particle size either to static annealing or to further melt-flow processing. Typical strategies developed in attempts to achieve immiscible blend compatibility include the following: the addition of block copolymers to the blend prior to melt processing, which has not led to commercial application [12], and reactive blending in which condensation-type functional groups on different polymer species undergo reaction at interfacial regions leading to the in situ production of block or graft copolymers, a method that has seen limited commercial application [13,14].

Recently, there has been growing interest in the application of mechanical alloying methods to the production of polymer blends, both miscible and immiscible, in the solid state [20–38]. Much of this research has involved the use of batch processes [20–31], including cryogenic and ambient high-energy ball milling as well as pan milling.

---

\* Corresponding author. Tel.: +1-847-491-7449; fax: +1-847-491-3728.  
E-mail address: j-torkelson@northwestern.edu (J.M. Torkelson).

Continuous mechanical alloying in the form of solid-state shear pulverization (SSSP) [32–38] has also been shown to yield positive results in overcoming many of the challenges associated with the melt processing of polymer blends. For example, pulverization has been shown to be useful in efficiently and intimately mixing polymer blends, both miscible and immiscible, where the components have an extreme viscosity ratio, eliminating phase inversion in systems in which the minority component is of much lower viscosity than the majority component [33,35]. Most recently, in situ compatibilization of several immiscible blends via pulverization has been demonstrated with the stabilization of the average dispersed-phase domain size to high-temperature annealing, i.e. stabilization to static coarsening [37]. In a complementary study, the in situ production of block copolymer via SSSP at interfacial regions in immiscible blends was demonstrated [38]. The block copolymer formation originates from the tunable scission of polymers during pulverization, leading to polymeric radicals that undergo interpolymer coupling reactions, providing proof for the hypothesis that in situ compatibilization during SSSP results from the presence of block copolymers formed during processing.

The demonstration of in situ blend compatibilization via pulverization without addition of compatibilization agents or functionalized polymers represents a significant achievement in overcoming a challenge associated with melt processing of blends, especially as it allows for control and retention of a particular dispersed-phase domain size upon further melt processing of the blend. However, as of yet, a quantitative comparison of the abilities of solid-state shear pulverization and melt processing to achieve small dispersed-phase particle sizes in the same blend has been lacking. Here we present such a study, employing several methods of comparison. In the first case, we have chosen to draw a comparison for a system in which melt mixing is expected to be unsuccessful in producing a sub-micron average dispersed-phase particle size. Additionally, we have undertaken comparison of a system that can yield sub-micron dispersed-phase particle sizes via melt mixing and demonstrate that pulverization can yield an even finer dispersion.

Quantitative comparison of results obtained by melt mixing with those obtained via pulverization is done in several ways. With a bimodal molecular weight (MW) polystyrene (PS)/polyethylene (PE) wax blend, comparison is made not only by morphological analysis via scanning electron microscopy (SEM) of blends made by SSSP and by melt mixing but also to the theoretical Taylor limit [39] for dispersed-phase droplet size obtainable by shear-flow processing. In 1934, Taylor [39] reported a relationship between the droplet diameter,  $D$ , and interfacial and shear forces in simple shear flow for a mix of a minor phase in a major phase, with both phases being Newtonian fluids:

$$D = \frac{4\Gamma(\eta_r + 1)}{\dot{\gamma}\eta_m\left(\frac{19}{4}\eta_r + 4\right)} \quad (1)$$

In Eq. (1),  $\dot{\gamma}$  is the shear rate,  $\eta_m$  is the matrix-phase viscosity,  $\eta_r = \eta_d/\eta_m$ , where  $\eta_d$  is the dispersed-phase viscosity, and  $\Gamma$  is the interfacial tension. The Taylor limit equation indicates that the final (minimum) droplet diameter achievable in shear flow is dependent on a competition between interfacial tension and shearing forces. It must be noted that the Taylor equation assumes that the droplets are perfectly spherical, no slip exists at the surface of the drop, and  $\eta_r < 2.5$ . Thus, while the Taylor equation has been found to be quantitative in its ability to predict droplet size for Newtonian fluids (in particular, it has been found to predict accurately the droplet diameters in Newtonian liquid mixtures with viscosity ratios between 0.1 and 1.0) [6], it often under predicts the dispersed-phase domain size achieved in typical high MW polymer blends, in which the dispersed-phase droplets encounter both elastic and viscous forces during mixing. For example, upon mixing a PS/polypolypropylene blend at a shear rate of  $\sim 65 \text{ s}^{-1}$ , Sundararaj and Macosko [15] found that the lowest achievable average dispersed-phase particle size was  $0.40 \mu\text{m}$ ; in contrast, the Taylor equation predicted a dispersed-phase diameter less than  $0.10 \mu\text{m}$ .

With a high-MW PS/high density polyethylene (HDPE) blend, comparison of dispersed-phase domain size is made here between samples prepared by pulverization and by melt processing. Analysis of morphology is achieved not only by SEM but also by characterization of crystallization behavior observed via differential scanning calorimetry (DSC). In general, semicrystalline polymers nucleate on existing heterogeneities such as catalyst debris or other impurities, and bulk crystallization occurs at temperatures slightly below the melt temperature,  $T_m$ . However, the phenomenon of fractionated crystallization [40–51] may occur in which a series of crystallization exotherms is observed via DSC as the result of the crystallization of different groups of droplets at independent supercoolings. The fractionated crystallization process has its origin in the specific interfacial energy difference,  $\Delta\gamma$ , between the polymeric chain and nucleating agent. Upon cooling a crystallizable polymer from the melt, the smallest  $\Delta\gamma$  value will initiate nucleation of the dispersed phase at the lowest supercooling, i.e. at the highest crystallization temperature. Crystal growth then occurs before reaching the supercooling associated with the heterogeneity possessing the second smallest  $\Delta\gamma$  value. However, if the dispersion is so fine that some droplets do not contain at least one heterogeneity active at the lowest supercooling, those droplets will crystallize either from a heterogeneity active at the second lowest supercooling or, in the instance, where no heterogeneity is present in the droplets, undergo homogeneous nucleation in which individual chain segments act as nucleating agents. Koutsky et al. [52] proved that the occurrence of successive crystallization steps was directly related to the size of the PE droplets dispersed in a matrix of silicon oil. In their experiments, the crystallization of the PE droplets during slow cooling (cooling rate =  $0.1 \text{ }^\circ\text{C/min}$ )

Table 1  
Viscosities of polymers used in Taylor limit experiments

Material	Viscosity at 180 °C and 125 s <sup>-1</sup> (Pa s)	Viscosity ratio ( $\eta_d/\eta_m$ )
PS	6.1	0.30
PE wax	1.8	

did not occur continuously but rather in separate stages initiated at distinctively different supercoolings.

## 2. Experimental

### 2.1. Materials

Experiments concerning the mixing of polymer blends utilized PE wax (Eastman Chemical Epolene C15 pellets, melt index = 4200 g/10 min at 190 °C/2.16 kg load as reported by the supplier) as the minor, dispersed phase and a moderate MW PS (Scientific Polymer Products; bimodal MW distribution PS flakes;  $M_n \sim 2000$  g/mol and  $M_w \sim 47,000$  g/mol as determined by gel permeation chromatography (GPC)). Blend compositions ranged from 1 to 15 wt% of the dispersed phase of PE wax. Experiments related to fractionated crystallization were done using a 95/5 wt% PS/HDPE blend (BASF; PS pellets;  $M_n = 110,000$  g/mol and  $M_w = 260,000$  g/mol as determined by GPC), (Equistar HDPE Petrothene LM6007; pellets; melt index = 0.8 g/10 min at 190 °C/2.16 kg load as reported by the supplier).

### 2.2. Rheological measurements

Viscosities of the polymers employed in the Taylor limit studies were determined via dynamic oscillatory shear experiments, using a Rheometric Scientific ARES Rheometer with 50 mm diameter parallel plates and a gap width of 0.41 mm. Temperature control was achieved through the use of a convection oven temperature controller. The Cox-Merz rule, relating linear viscoelastic properties to the steady shear viscosity, allowed for the use of oscillatory shear data to determine viscosities at a shear rate equal to  $\sim 125$  s<sup>-1</sup>, the shear rate reported [53] as a typical shear rate for the conditions used in the Haake Rheocord System 40 batch mixer. The viscosity of the PE wax sample was independent of shear rate for all conditions tested, indicating that the PE wax was a Newtonian fluid. The PS sample was found to begin shear-thinning behavior at a shear rate of  $\sim 1$  s<sup>-1</sup>, and exhibited a power-law index ( $n$ ) of 0.76, indicating weak pseudoplastic behavior. Viscosity data are given in Table 1.

### 2.3. Melt mixing

PS/PE wax blends were melt mixed for 10 min using a Haake Rheocord System 40 batch, intensive melt mixer

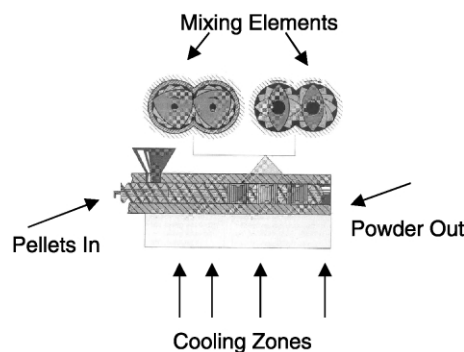


Fig. 1. Schematic of apparatus used for solid-state shear pulverization.

equipped with Banbury blades. Torque versus time data revealed a torque plateau at  $\sim 2$  min, indicative of an equilibrium in the final blend morphology being reached after this time. The 55 g of pellets were fed to the mixer operating at 180 °C and 50 rpm, yielding a reported [53] typical shear rate of  $\sim 125$  s<sup>-1</sup>. PS/HDPE blends were produced via melt mixing using a Berstorff co-rotating twin-screw extruder operating at 200 rpm and a melt temperature of  $\sim 215$  °C.

### 2.4. Pulverization

PS/PE wax and PS/HDPE blends were initially dry blended (hand mixing of pellets or flakes) and then processed using a Berstorff pulverizer (for a schematic, see Fig. 1) operating at a screw speed of 200 rpm using a screw configuration designed to provide substantial shear to the polymer. Feed rates were  $\sim 0.45$  kg/h (99/1, 95/5, and 90/10 wt% PS/PE wax blends),  $\sim 0.34$  kg/h (85/15 wt% PS/PE wax blend) or  $\sim 0.11$  kg/h (95/5 wt% PS/HDPE blend). Further information regarding pulverization, including equipment description, is given in Refs. [32–36].

### 2.5. Differential scanning calorimetry

A Perkin–Elmer DSC-7 differential scanning calorimeter was used for thermal analysis of the PS/HDPE blends. The crystallization temperature,  $T_c$ , of the HDPE phase was measured by holding each sample for 3 min at 170 °C, followed by cooling each sample from 170 to 20 °C at 10 °C/min. The values of  $T_c$  reported here represent the onset of crystallization exotherm peaks.

### 2.6. Morphological characterization

A Hitachi S3500N scanning electron microscope, operating at a 10 kV accelerating voltage, was used to observe blend morphology. SEM sample preparation consisted of fracturing samples, obtained either directly from the batch mixer or from impact testing bars, the latter made for pulverized blends and twin-screw extruded blends by injection molding. The fracture surface was then coated

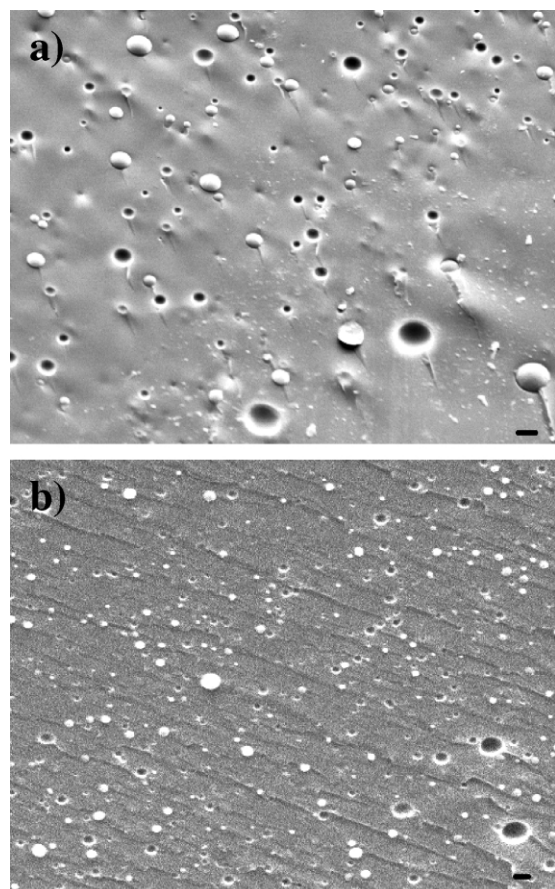


Fig. 2. SEM micrograph comparison for 95/5 wt% PS/PE wax blends prepared by (a) batch, intensive mixing and (b) SSSP. Sizebar, 3  $\mu\text{m}$  in (a); sizebar, 2  $\mu\text{m}$  in (b).

with a 3.5 nm layer of gold using a Cressington 208HR high-resolution coater in order to minimize sample charging effects due to the electron beam. The number-average dispersed-phase domain diameter,  $D_n$ , was determined by characterizing 200 to 600 particles per sample using Scion Image Beta 4.0.2 image analysis software to determine the area of each particle. No attempt was made to correct errors in  $D_n$  values associated with the fact that a fracture surface may yield apparent particle sizes that differ from true particle diameters because of the non-spherical nature of some particles or the possibility that a particle was sectioned at a location other than its center. Sundararaj and Macosko [15] have shown that differences of less than 10% result in the average particle size when accounting for such factors and that trends in the results are unaffected by such corrections.

### 3. Results and discussion

#### 3.1. PS/PE wax blend: comparison of dispersion via SSSP to the Taylor limit for melt mixing

The PS/PE wax blend was selected for study as, based on Eq. (1), it was expected to allow for the production of a

number-average dispersed-particle size via melt mixing that substantially exceeded 1  $\mu\text{m}$ . Employing the viscosity data in Table 1, shear rate information provided by the manufacturer of the batch, intensive melt mixer, and an interfacial tension value of 5.8 mN/m [54], the Taylor equation predicts a value of  $D_n$  of 7.3  $\mu\text{m}$ . This value assumes that all mixing occurs via shear flow and that there is no contribution of coalescence to the observed dispersed-phase domain size. Elongational flow effects, present in a batch, intensive melt mixer, would tend to result in a smaller particle size, while the effect of particle coalescence, expected at higher minor phase content during melt mixing, would tend to result in a larger particle size than predicted by the Taylor equation.

Fig. 2 compares the observed morphologies for a 95/5 wt% PS/PE wax blend subjected to processing via melt mixing or pulverization. It is clear from Fig. 2 that the number-average dispersed-phase diameters of the melt-mixed blend ( $D_n = 3.0 \mu\text{m}$ ) and of the pulverized blend ( $D_n = 0.7 \mu\text{m}$ ) are less than that predicted by the Taylor equation ( $D_n = 7.3 \mu\text{m}$ ). Thus, in the very low dispersed-phase concentration regime, both polymer-processing operations are able to produce blends having dispersed-phase domain sizes that are smaller by at least a factor of 2 than the predicted Taylor limit. However, SSSP produces a blend with a value of  $D_n$  that is an order of magnitude below that predicted by Eq. (1). For the melt-mixed blend, the difference between the calculated Taylor limit and the observed  $D_n$  value may be attributed in part to the presence of extensional flow in the batch mixer; the presence of such flow has been shown to produce finer dispersions than pure, simple shear flows [6,55]. Additionally, there is a range of shear rates present in the batch, intensive melt mixer, leading to some inaccuracy when using Eq. (1) with a single shear rate value. Furthermore, the PS exhibits slightly non-Newtonian flow behavior at shear rates found in the mixing, adding to further inaccuracy associated with use of Eq. (1). Nonetheless, pulverization produces a dispersed phase with an average particle diameter that is a much smaller than predicted either by the Taylor equation or observed experimentally from intensive melt mixing.

Fig. 3 compares the dispersion achieved upon increasing the minor-phase PE wax concentration to 10 wt%. As compared with the 95/5 wt% PS/PE wax blend, there is an approximate doubling of the average dispersed-phase domain size in the 90/10 wt% melt-mixed system, with  $D_n$  increasing to 6.6  $\mu\text{m}$ . The growth in  $D_n$  at higher concentration of the dispersed phase undoubtedly results from flow-induced coalescence that occurs in blends of higher minor-phase content prepared by melt mixing. In contrast to the flow-induced coalescence effects occurring in the melt mixed blend,  $D_n$  of the pulverized sample remains at 0.7  $\mu\text{m}$  in the 90/10 wt% PS/PE wax blend, identical to the result obtained in the 95/5 wt% PS/PE wax blend. While pulverization subjects the blend to repeated fragmentation and fusion cycles, the solid-state nature of the process



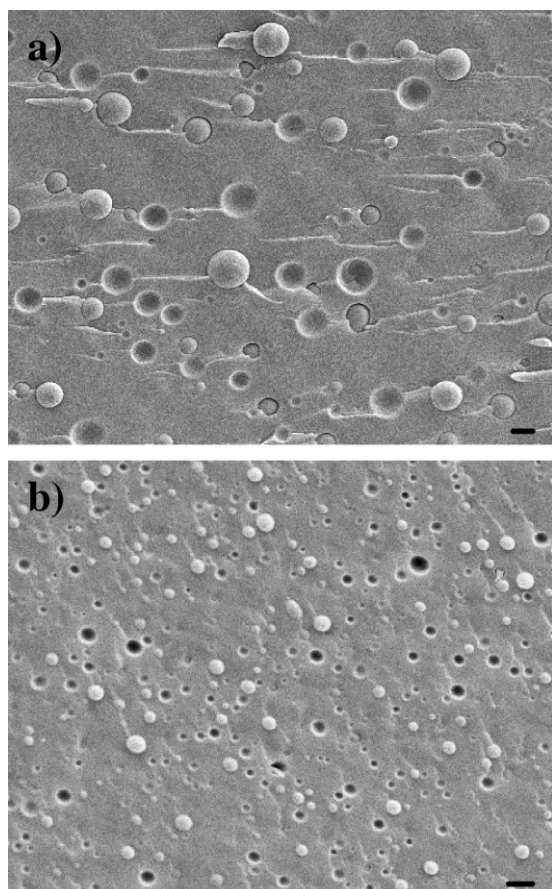


Fig. 3. SEM micrograph comparison for 90/10 wt% PS/PE wax blends prepared by (a) batch, intensive mixing and (b) SSSP. Sizebar, 10  $\mu\text{m}$  in (a); sizebar, 2  $\mu\text{m}$  in (b).

disallows coalescence effects, resulting in the dispersed-phase diameters in the 95/5 and 90/10 wt% PS/PE wax blends being equal.

Fig. 4 illustrates the morphologies observed in both melt mixed and pulverized PS/PE wax blends containing 15 wt% PE wax, a dispersed-phase concentration more typical of commercial blending applications. Regarding the melt mixed sample, the increase in the number-average dispersed-phase diameter to 17.5  $\mu\text{m}$  is indicative of the increasing importance of coalescence during melt processing of blends with higher dispersed-phase content. However, the pulverized 85/15 wt% PS/PE wax blend yields an average dispersed-phase particle size of 0.6  $\mu\text{m}$ , within error identical to that produced via pulverization of the 90/10 and 95/5 wt% PS/PE wax blends and nearly a factor of 30 smaller than that obtained in the analogous melt-mixed blend. This is an indication that, with the use of certain pulverization conditions and blend components, it is possible via SSSP to obtain number-average dispersed-phase particle sizes that are independent of minor-phase content over a range of composition that results in substantial coalescence effects during melt-state processing.

Fig. 5 provides a graphical summary of the number-average dispersed-phase diameter as a function of

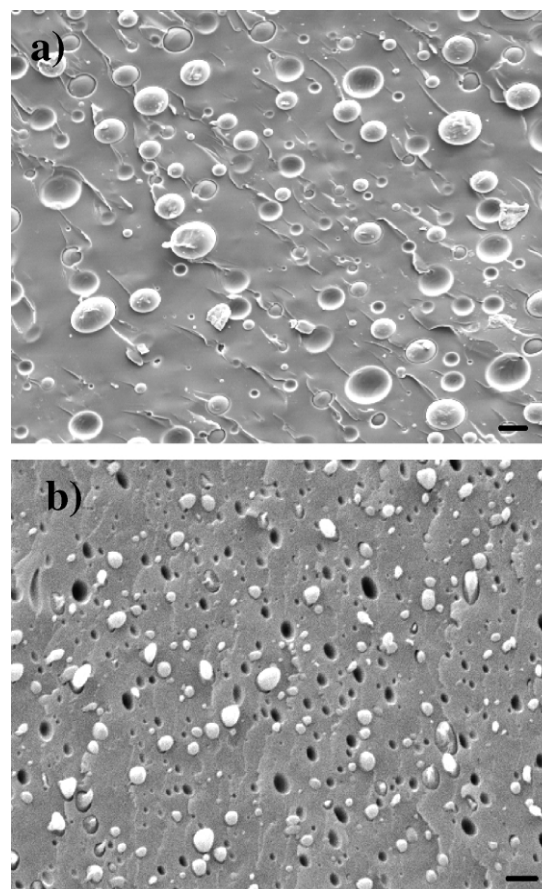


Fig. 4. SEM micrograph comparison for 85/15 wt% PS/PE wax blends prepared by (a) batch, intensive mixing and (b) SSSP. Sizebar, 25  $\mu\text{m}$  in (a); sizebar, 2  $\mu\text{m}$  in (b).

dispersed-phase concentration for both the melt mixed and pulverized PS/PE wax blends, in addition to the calculated Taylor limit. Included in Fig. 5 are results for a 99/1 wt% PS/PE wax blend. (While values of  $D_n$  were obtained for this system from analysis of a series of SEM micrographs, the very ‘dilute’ nature of the dispersed phase did not allow for inclusion of single micrographs representative of the pulverized or melt-mixed blends.) It is noteworthy that the

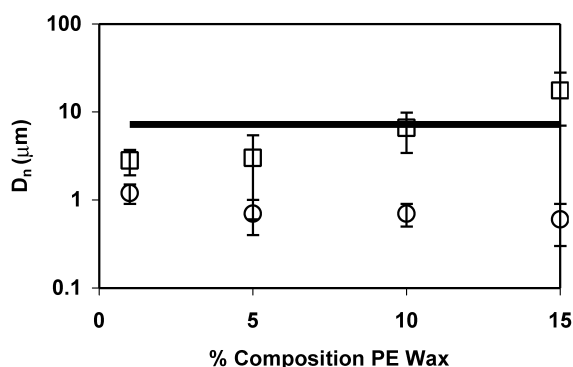


Fig. 5. Comparison of  $D_n$  for PS/PE wax blends prepared by (□) batch, intensive mixing, and (○) SSSP relative to the predicted (—) Taylor limit. Error bars indicate the breadth in particle size (one standard deviation from mean), not measurement errors.

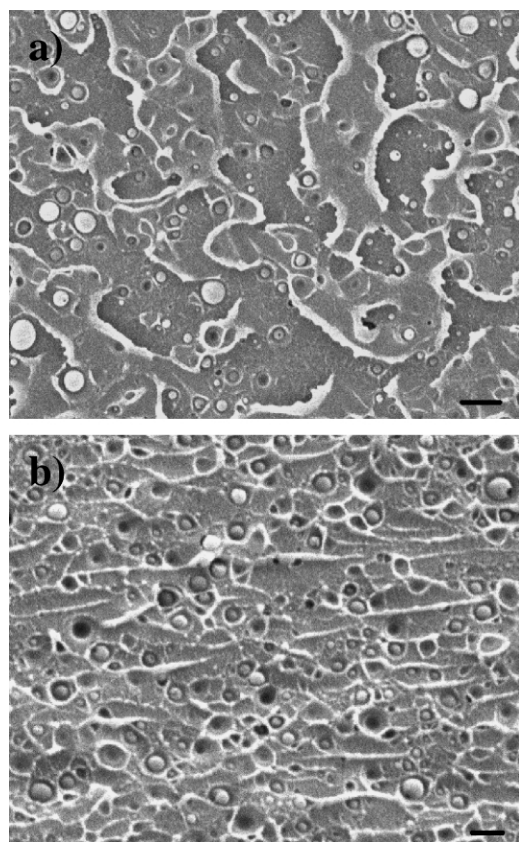


Fig. 6. SEM micrograph comparison for 95/5 wt% PS/HDPE blend prepared by (a) twin-screw extrusion and (b) SSSP. Sizebar, 2  $\mu\text{m}$  in (a); sizebar, 1  $\mu\text{m}$  in (b).

$D_n$  values obtained in the 99/1 and 95/5 wt% pulverized blends are similar as are the values of  $D_n$  obtained in the 99/1 and 95/5 wt% melt-mixed blends. The similarity in the melt-mixed blends is due to the lack of substantial coalescence effects during melt mixing of low dispersed-phase content blends; the similarity in the pulverized blends is yet a further indication of the ability of pulverization to yield very small dispersed-phase particle size independent of minor-phase content over a substantial range of composition.

It must be noted that the ‘error bars’ shown in Fig. 5 do not represent ‘error’ but instead indicate the breadth in particle size (one standard deviation from the mean), and thus provide a measure of the particle-size distribution. Fig. 5 therefore shows that the particle size at one standard deviation above the mean is in the range of 0.9 to 1.5  $\mu\text{m}$  in the pulverized blends. In contrast, with the exception of the 95/5 wt% PS/PE wax blend, the particle size at one standard deviation below the mean for the melt mixed blends ranges from 1.9 to 7  $\mu\text{m}$ . Although the mean dispersed-phase particle size is nearly the same in the 99/1 and 95/5 wt% PS/PE wax blends prepared by melt mixing, the breadth of the distribution increases dramatically at the higher dispersed-phase concentration, indicating the presence of a number of much larger particles in the 95/5 wt% PS/PE wax blend.

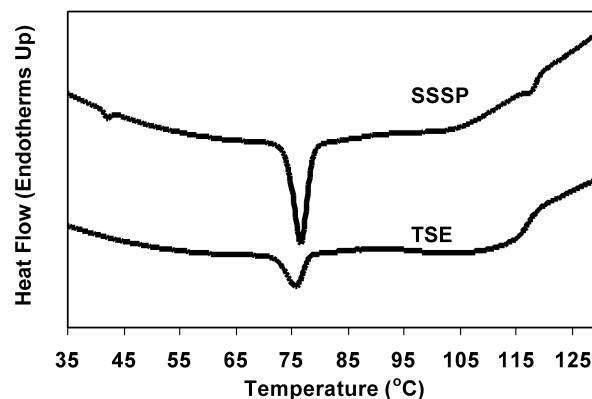


Fig. 7. DSC comparison of crystallization behavior (measurements upon cooling) for 95/5 wt% PS/HDPE blends prepared by SSSP and twin-screw extrusion (TSE).

Such effects are absent in the PS/PE wax blends prepared by pulverization, suggesting that pulverization has a technological advantage over melt mixing in producing blends with optimal mechanical properties that rely on dispersed-phase particles being below a critical size.

### 3.2. PS/HDPE blend: fractionated crystallization comparison of dispersion via pulverization to that via melt mixing

Fig. 6 compares the morphologies obtained for a 95/5 wt% PS/HDPE blend processed either by twin-screw extrusion or by pulverization. It is evident from Fig. 6 that, regardless of the processing method, sub-micron dispersions are produced for both blends. Quantitative analysis of SEM micrographs reveals that the melt-mixed blend yields a value of  $D_n = 500$  nm while the pulverized blend yields a value of  $D_n = 270$  nm, indicating that pulverization of a PS/HDPE blend can produce an average dispersed-phase diameter that is a factor of 2 smaller than that achieved via intensive melt mixing. It is noteworthy that the nanoscale value of  $D_n$  obtained in the pulverized blend is at most several times the resolution limit achievable with the scanning electron microscope used in this study. Thus, it is useful to employ an alternative method of comparing the dispersion achievable via pulverization and melt mixing in order to differentiate further the morphologies produced by each processing method.

The fractionated crystallization behavior of the semi-crystalline HDPE provides a second method of characterizing the fineness of dispersion achieved in PS/HDPE blends produced by melt mixing or SSSP. Fig. 7 shows the fractionated crystallization data obtained using DSC for the 95/5 wt% PS/HDPE blends produced by twin-screw extrusion or by pulverization. Major differences are apparent in both the relative size and number of crystallization exotherms present in each blend. Specifically, crystallization exotherms with onset temperatures of  $\sim 79$ – $80$  and  $\sim 119$   $^{\circ}\text{C}$  are present in both blends, with the latter

representing crystallization associated with heterogeneities active at the lowest supercooling. Additionally, there is a third, small crystallization exotherm present in the pulverized blend, with an onset temperature of  $\sim 43^\circ\text{C}$ , that is absent in the melt-mixed blend. Analysis of the area associated with each exotherm indicates a huge difference in the relative level of crystallization that occurs at each supercooling depending on how the blend was made. In the case of the blend processed via twin-screw extrusion, the exotherm at  $119^\circ\text{C}$  accounted for  $\sim 76\%$  of the crystallization while the exotherm at  $79\text{--}80^\circ\text{C}$  accounted for  $\sim 24\%$  of the crystallization. In contrast, the finer dispersion in the pulverized blend led to a major decrease in the crystallinity associated with the exotherm at  $119^\circ\text{C}$  ( $\sim 11\%$  of the crystallization) and a major increase in that at  $79\text{--}80^\circ\text{C}$  ( $\sim 85\%$  of the crystallization). Additionally,  $\sim 4\%$  of the crystallization observed in the pulverized blend occurred at an onset  $T_c$  of  $43^\circ\text{C}$ . Given the results of previous studies [40–51] of fractionated crystallization in multi-phase polymeric systems, the overall shift of crystallization to lower temperature in the pulverized blend corroborates the conclusion from the SEM data (Fig. 6) that pulverization is capable of producing a more finely dispersed blend than that made by twin-screw extrusion.

There is a possibility that the very small crystallization exotherm present in the pulverized blend at an onset temperature of  $43^\circ\text{C}$  may represent homogeneous nucleation, which is expected to occur only in dispersed phase regions of nanoscopic dimension, sufficiently small to allow for the absence of impurities promoting heterogeneous nucleation. It has been suggested [40,43,47] that the theoretical homogeneous nucleation temperature,  $T_{\text{homo}}$ , may be calculated according to the relation  $T_{\text{homo}} = 0.8T_m^\circ$ , where  $T_m^\circ$  is the equilibrium melting temperature, i.e. the melting temperature (in K) of a perfect polyethylene crystal. Using literature values for  $T_m^\circ$  ranging from  $141\text{--}145^\circ\text{C}$  [56,57],  $T_{\text{homo}}$  would be expected to be  $\sim 60^\circ\text{C}$ , relatively close to the exotherm observed at  $43^\circ\text{C}$ . Unfortunately, the very small level of crystallization at  $43^\circ\text{C}$  disallows experiments confirming the homogeneous or heterogeneous nature of the nucleation. Further investigation should be undertaken with other blends to determine whether pulverization can lead to a nanoscopically fine dispersion that yields homogeneous nucleation of crystallization.

### 3.3. Absence or presence of chain scission accompanying pulverization

Some discussion regarding the mechanochemical events accompanying blend pulverization is warranted. Previous work [37] has shown that compatibilized PS/HDPE and PS/poly(methyl methacrylate) (PMMA) blends may be produced via pulverization. In that study, it was hypothesized that compatibilization originated from the in situ formation of block copolymer produced from the interpolymer coupling of macroradicals created from the polymer chains

cleaved during SSSP; GPC analysis revealed small to moderate reductions in the PS MW in the pulverized blends relative to the PS MW before pulverization, proving the presence of chain cleavage during SSSP. Furthermore, a complementary study [38] has conclusively demonstrated the presence of block copolymer produced via interpolymer coupling of polymeric radicals resulting from chain scission during pulverization of PS/PMMA blends. Thus, when blend compatibilization is the goal, the achievement of small to moderate levels of chain scission during SSSP is important.

However, the results from the present study show that pulverization does not necessarily result in chain scission and that the occurrence of chain scission during pulverization is not in general a prerequisite for the attainment of sub-micron dispersed-phase domain size in blends. GPC analysis of the pre- and post-SSSP bimodal PS employed in the PS/PE wax, Taylor limit study revealed little or no reduction in MW within error while similar analysis of the PS used in the PS/HDPE, fractionated crystallization study showed reductions of 53 and 54% in  $M_n$  and  $M_w$ , respectively, after pulverization. The low MW of the bimodal PS sample used in the Taylor limit study, with  $M_n \sim 2000$  g/mol and  $M_w \sim 47,000$  g/mol, indicates that there is little likelihood of chain entanglement in the bimodal PS sample. (The MW between chain entanglements in PS has been estimated from rheological properties be 18,000 g/mol [58].) Previous studies [32,38] have shown that little or no chain scission of PS is achieved via SSSP when the PS is of sufficiently low MW to be unentangled, a result that can be understood based on the ability of unentangled chains to undergo chain pullout exclusively during fracture or fragmentation [59,60]. In contrast, the substantial chain scission achieved during pulverization of the PS/HDPE blend may be explained by the fact that the PS used in the fractionated crystallization study is well above the entanglement MW; when entangled polymers undergo fracture or fragmentation, the chains may experience chain scission rather than chain pullout [59,60]. Thus, in contrast to the important role of mechanochemistry for the achievement of blend compatibilization via pulverization, the achievement of sub-micron dispersed phase domain sizes via pulverization of blends does not in general rely on the level of mechanochemistry accompanying the process.

## 4. Conclusions

This study provides the first quantitative comparison of the abilities of solid-state shear pulverization and melt processing to achieve small dispersed-phase particle sizes in the same blend. For a PS/PE wax system in which melt mixing was expected to be unsuccessful in producing sub-micron dispersed-phase particle sizes, pulverization produced a sub-micron dispersion of PE wax in blends containing up to 15 wt% of the dispersed phase.



Furthermore, solid state processing rendered coalescence effects irrelevant, and the mean particle size remained nearly uniform over a 1 to 15 wt% composition range of the dispersed phase. Conversely, evidence of strong coalescence effects were manifested by a large increase in the mean dispersed-phase diameters with increasing minor-phase content in PS/PE wax blends prepared in a batch, intensive melt mixer;  $D_n$  of the pulverized and melt mixed blends differed by as much as a factor of  $\sim 30$  when 15 wt% of the dispersed phase was employed. Additionally, sub-micron average dispersed-phase domain size was obtained in PS/HDPE blends processed either by SSSP or twin-screw extrusion, with pulverization yielding a  $D_n$  value of approximate one-half that obtained by extrusion. Complementary analysis of the fractionated crystallization behavior of the HDPE phase confirmed that the pulverized blend yielded a much finer dispersion than that associated with the melt-mixed blend, as evidenced by an overall shift to lower crystallization temperatures in the pulverized blend. Finally, the combined results of the bimodal PS/PE wax and the PS/HDPE studies prove that the production of finely-dispersed blends via SSSP is in general not related to the achievement of pulverization-induced mechanochemistry such as chain scission.

## Acknowledgements

This work was supported by Material Sciences Corporation and by the NSF-MRSEC program (Grant DMR-0076097) at the Materials Research Center of Northwestern University.

## References

- [1] Utracki LA. Polymer alloys and blends. Munich: Hanser; 1989.
- [2] Scott CE, Macosko CW. Polymer 1995;36:461–70.
- [3] Favis BD, Therrien D. Polymer 1991;32:1474–81.
- [4] Takeda Y, Keskkula H, Paul DR. Polymer 1992;33:3173–81.
- [5] Lepers JC, Favis BD. AIChE J 1999;45:887–95.
- [6] Grace HP. Chem Engng Commun 1982;14:225–77.
- [7] Scott CE, Joung SK. Polym Engng Sci 1996;36:1666–74.
- [8] Utracki LA, Shi ZH. Polym Engng Sci 1992;32:1824–33.
- [9] Fayt R, Jerome R, Teyssie P. Makromol Chem 1986;187:837–52.
- [10] Liu NC, Xie HQ, Baker WE. Polymer 1993;34:4680–7.
- [11] Su Y, Min KS, Quirk RP. Polymer 2001;42:5121–34.
- [12] Koning C, Van Duin M, Pagnoulle C, Jerome R. Prog Polym Sci 1998;23:707–57.
- [13] Paul DR, Bucknall CB. Polymer blends. New York: Wiley; 2000. vol. 1 and 2.
- [14] Weber M. Macromol Symp 2002;181:189–200.
- [15] Sundararaj U, Macosko CW. Macromolecules 1995;29:2647–57.
- [16] Zumbunnen DA, Chhibber C. Polymer 2002;43:3267–77.
- [17] Lyu SP, Bates FS, Macosko CW. AIChE J 2002;48:7–14.
- [18] Datta A, Baird DG. Polymer 1995;36:505–14.
- [19] Gray MK, Kinsinger MI, Torkelson JM. Macromolecules 2002;35:8261–4.
- [20] Ishida T. J Mater Sci Lett 1994;13:623–8.
- [21] Pan J, Shaw WJD. J Appl Polym Sci 1994;507–14.
- [22] Shaw WJD. Mater Sci Forum 1998;269(2):19–29.
- [23] Smith AP, Bai C, Ade H, Spontak RJ, Balik CM, Koch CC. Macromol Rapid Commun 1998;19:557–61.
- [24] Smith AP, Ade H, Balik CM, Koch CC, Smith SD, Spontak RJ. Macromolecules 2000;33:2595–604.
- [25] Smith AP, Spontak RJ, Koch CC, Smith AD, Ade H. Macromol Mater Engng 2000;274:1–12.
- [26] Smith AP, Ade H, Koch CC, Smith SD, Spontak RJ. Macromolecules 2000;33:1163–72.
- [27] Smith AP, Ade H, Koch CC, Spontak RJ. Polymer 2001;42:4453–7.
- [28] Smith AP, Ade H, Smith SD, Koch CC, Spontak RJ. Macromolecules 2001;36:1536–8.
- [29] Cavalieri F, Padella F, Bourbonneux S. Polymer 2002;43:1155–61.
- [30] Font J, Muntasell J, Cesari E. Mater Res Bull 1999;34:157–65.
- [31] Chen Z, Wang Q. Polym Int 2001;50:966–72.
- [32] Furgiele N, Lebovitz AH, Khait K, Torkelson JM. Macromolecules 2000;33:225–8.
- [33] Furgiele N, Lebovitz AH, Khait K, Torkelson JM. Polym Engng Sci 2000;40:1447–57.
- [34] Khait K, Torkelson JM. Polym-Plast Technol 1999;38:445–57.
- [35] Khait K, Torkelson JM. Int Polym Proc 2000;15:343–7.
- [36] Ganglani M, Torkelson JM, Carr SH, Khait K. J Appl Polym Sci 2001;80:671–9.
- [37] Lebovitz AH, Khait K, Torkelson JM. Macromolecules 2002;35:8672–5.
- [38] Lebovitz AH, Khait K, Torkelson JM. Macromolecules 2002; in press.
- [39] Taylor GI. Proc Roy Soc 1934;A146:501–23.
- [40] Frensch H, Harnischfeger P, Jungnickel BJ. ACS Symp Ser 1989;395:101–25.
- [41] Avella M, Martuscelli E, Raimo M. Polymer 1993;34:3234–40.
- [42] Tang T, Huang BT. J Appl Polym Sci 1994;53:355–60.
- [43] Santana OO, Muller AJ. Polym Bull 1994;32:471–7.
- [44] Morales RA, Arnal ML, Muller AJ. Polym Bull 1995;35:379–86.
- [45] Balsamo V, vonGyldenfeldt F, Stadler R. Macromol Chem Phys 1996;197:3317–41.
- [46] Arnal ML, Muller AJ. Macromol Chem Phys 1999;200:2559–76.
- [47] Everaert B, Groeninckx G, Aerts L. Polymer 2000;41:1409–28.
- [48] Chen HL, Hsiao SC, Lin TL, Yamauchi K, Hasegawa H, Hashimoto T. Macromolecules 2001;34:671–4.
- [49] Nojima S, Toei M, Hara S, Tanimoto S, Sasaki S. Polymer 2002;43:4087–90.
- [50] Muller AJ, Balsamo V, Arnal ML, Jakob T, Schmalz H, Abetz V. Macromolecules 2002;35:3048–58.
- [51] Loo YL, Register RA, Ryan AJ. Phys Rev Lett 2000;84:4120–3.
- [52] Koutsky JA, Walton AG, Baer E. J Appl Phys 1967;38:1832–9.
- [53] Dieter S. Haake representative. Personal communication.
- [54] Chen CC, White JL. Polym Engng Sci 1993;33:923–30.
- [55] Karam HJ, Bellinger JC. Ind Engng Chem Fundam 1968;7:576–81.
- [56] Wunderlich B. Thermal analysis. New York: Academic Press; 1990.
- [57] Fatou JG. In: Vasile C, Seymour RB, editors. Melting of polyolefins in handbook of polyolefins. New York: Marcel Dekker; 1993.
- [58] Majeste JC, Montfort JP, Allal A, Marin G. Rheol Acta 1998;37:486–99.
- [59] Washiyama J, Kramer EJ, Creton CF, Hui CY. Macromolecules 1994;27:2019–24.
- [60] Sambasivam M, Klein A, Sperling LH. J Appl Polym Sci 1995;58:357–66.